# Trovacene Chemistry, 3[+]

# The Mono-, Di-, and Tri([5]trovacenyl)boranes: A Study of Intermetallic Communication Across an $sp^2$-Hybridized Boron Atom

**Christoph Elschenbroich,*[a] Matthias Wolf,[a] Olaf Burghaus,[a] Klaus Harms,[a] and Jürgen Pebler[a]**

*Dedicated to Professor Christoph Rüchardt on the occasion of his 70th birthday*

**Keywords:** EPR spectroscopy / Metallocenylboranes / Organovanadium radicals / Redox chemistry (CV) / X-ray diffraction

The paramagnetic complexes di(mesityl)([5]trovacenyl)-borane (**5**$^{\cdot}$), (mesityl)di([5]trovacenyl)borane (**6**$^{\cdot\cdot}$), and tri([5]trovacenyl)borane (**7**$^{\cdot\cdot\cdot}$) were prepared from [5]trovacenyllithium, ($\eta^5$-$C_7H_7$)V($\eta^5$-$C_5H_4$Li), and $(Mes)_2BF$, $(Mes)BF_2$, and $BF_3$, respectively. The propeller-shaped species **5**$^{\cdot}$, **6**$^{\cdot\cdot}$, and **7**$^{\cdot\cdot\cdot}$ were subjected to X-ray diffraction with the aim of possibly correlating the twist angles with intramolecular intermetallic communication. Cyclic voltammetry points to successive vanadium-centered oxidation processes and boron-centered reduction, a small redox splitting $\delta E_{1/2}$[(2+/+), (+/0)] being observed for **6**$^{\cdot\cdot}$. According to EPR spectroscopy, performed in fluid solution, the exchange interaction $J$ in the diradical **6**$^{\cdot\cdot}$ approaches the fast-exchange region and is attenuated significantly by quaternization at boron in [**6**$^{\cdot\cdot}$–*n*Bu]$^-$. Although EPR spectroscopy of the triradical **7**$^{\cdot\cdot\cdot}$ also indicates an extensive exchange interaction, the exchange parameters, derived from spectral simulation, follow the gradation $J$(**7**$^{\cdot\cdot\cdot}$) $\approx$ 1/3 $J$(**6**$^{\cdot\cdot}$). The magnetic susceptibility of **6**$^{\cdot\cdot}$ and **7**$^{\cdot\cdot\cdot}$ follows the same trend. As expected, compound **7**$^{\cdot\cdot\cdot}$ exhibits spin frustration because it contains three antiferromagnetically coupled $S$ = 1/2 systems that are arranged in an equilateral triangle.

## Introduction

The screening of diverse inorganic and organic groups for their potential as spacers, capable of mediating electronic and magnetic interactions between metal centers, remains a topic of intense investigation.[2] With this aim in mind, we previously prepared the half-sandwich complexes $Mes_2B[(\eta^6\text{-Mes})Cr(CO_3)]$ (**1**), $MesB[(\eta^6\text{-Mes})Cr(CO)_3]_2$ (**2**), and $B[(\eta^6\text{-Mes})Cr(CO)_3]_3$ (**3**), determined their molecular structures by X-ray diffraction, and studied their IR-, redox-, and EPR properties.[3]

Structurally, these propeller-shaped complexes differ in the dihedral angle between the $\eta^6$-arene planes and the reference plane which is spanned by the three carbon atoms bonded to boron. If interactions between these complex moieties were governed by conjugation between the aromatic π-systems and the vacant $p_z$ orbital of the boron atom, compounds **1**, **2**, and **3** would be expected to exhibit characteristic spectral and electrochemical differences. However, IR spectroscopy and cyclic voltammetry indicated almost no discernible communication between the $Cr(CO)_3$ units of either **2** or **3**. A more sensitive tool for probing intramolecular communication is provided by EPR spectroscopy, which may either be applied to mixed valence species, to search for spin delocalization, or it may be used for oligoradicals, to assess the extent of exchange coupling. We have used both methods in the past for related cases;[1][4] they failed for **1**–**3**, however, because the requisite paramagnetic species could not be obtained either chemically or electrochemically.

Our recent research[1][5] with the paramagnetic, neutral complex ($\eta^7$-$C_7H_7$)V($\eta^5$-$C_5H_5$) (**4**$^{\cdot}$) [or trovacene, for ($\eta^7$-tropylium)vanadium($\eta^5$-cyclopentadienyl)[6]] caused us to synthesize the mono-, di-, and tri([5]trovacenyl)boranes **5**$^{\cdot}$–**7**$^{\cdot\cdot\cdot}$ in order to study their electrochemical and EPR spectroscopic characteristics. The redox splitting $\delta E_{1/2}$, i.e., the difference in the potentials of subsequent redox steps, as well as the exchange coupling constant $J$, for diradical **6**$^{\cdot\cdot}$ and triradical **7**$^{\cdot\cdot\cdot}$, should both provide information on the extent of intermetallic communication via the central boron atom. The results from this investigation should also complement those obtained previously for the related complex tri(ferrocenyl)borane, $[(\eta^5\text{-}C_5H_5)(\eta^5\text{-}C_5H_4)Fe]_3B$ (**8**).[7]

## Results and Discussion

### Synthesis

Trovacene undergoes selective monolithiation at the cyclopentadienyl ring.[8][9] Subsequent reaction with the B–F functionality affords di(mesityl)([5]trovacenyl)borane

[+] Part 2: Ref.[1]

[a] Fachbereich Chemie der Philipps-Universität Marburg, Hans-Meerwein-Strasse, D-35032 Marburg, Germany
Fax: (internat.) +49-(0)6421/28-28917
E-mail: eb@ps1515.chemie.uni-marburg.de

  1434–1948/99/1212–2173 $ 17.50+.50/0 

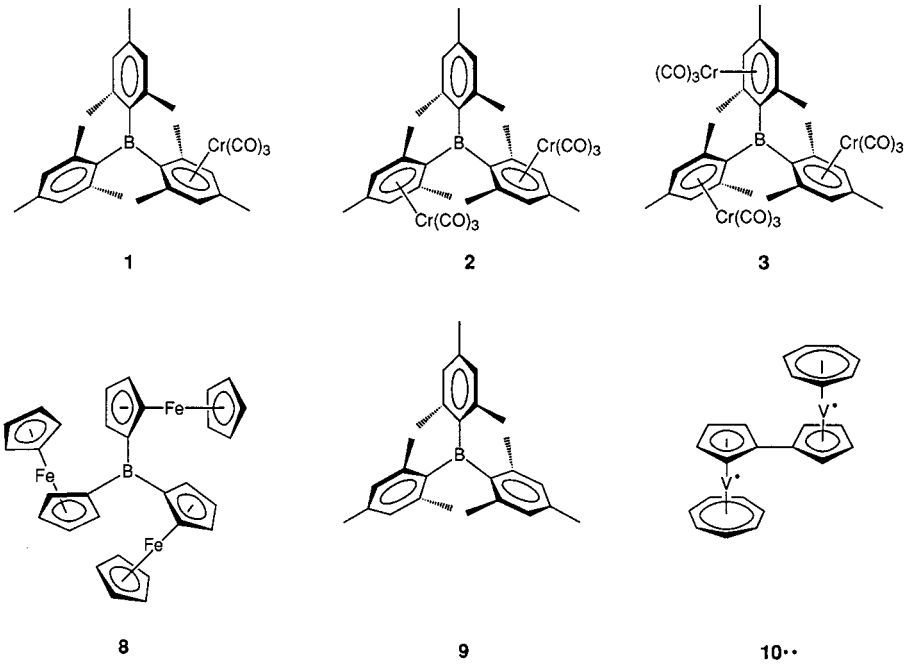


1 2 3 8 9 10••

(**5**•), (mesityl)di([5]trovacenyl)borane (**6**••) and tri([5]trovacenyl)borane (**7**•••) (Scheme 1). The mesityl group was chosen as an auxiliary ligand to sterically protect the boron atom in order to improve the kinetic stability of $R_3B$ anions,[10] which are also targets of the present investigation. Compounds **5**• and **6**•• crystallized as green cubes, and **7**••• formed green needles. The solubility in aromatic solvents decreases in the order **5**• > **6**•• > **7**•••.

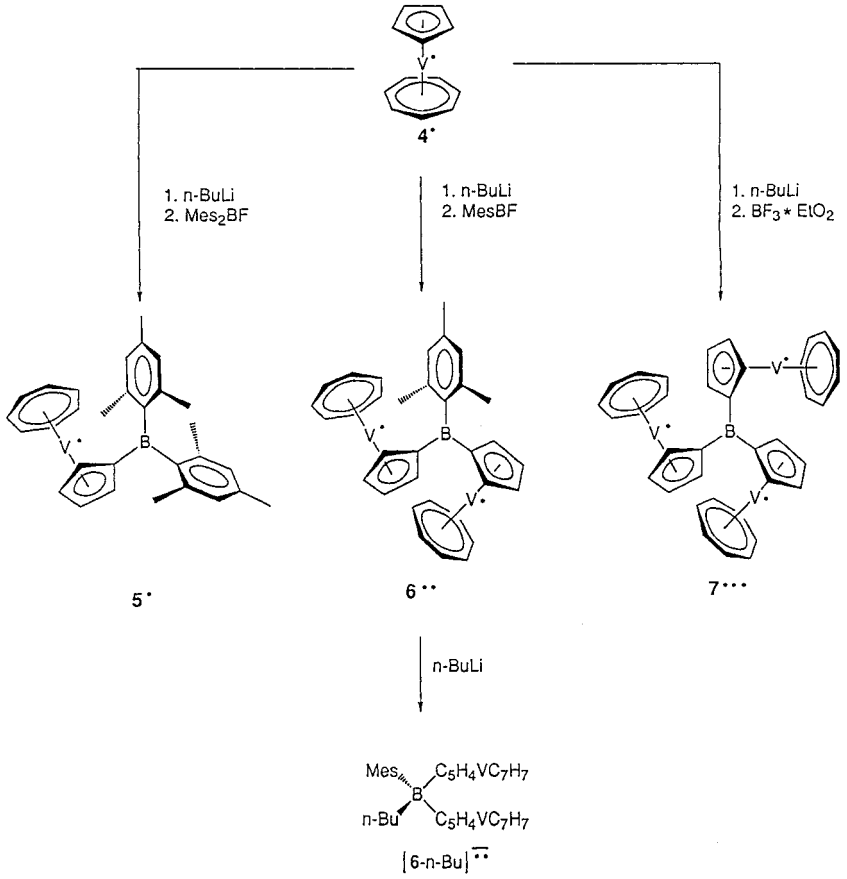


Scheme 1

### Molecular Structures of $5^{\cdot}$, $6^{\cdot\cdot}$, and $7^{\cdot\cdot\cdot}$ in the Crystal

While it may not be assumed that the structures of $\mathbf{5}^{\cdot}-\mathbf{7}^{\cdot\cdot\cdot}$ in the solid state are identical to those in fluid solution, where CV and EPR spectroscopic studies are performed, X-ray diffraction studies were nevertheless carried out to extract trends in the torsional angles which characterize these molecules. The structures of $\mathbf{5}^{\cdot}-\mathbf{7}^{\cdot\cdot\cdot}$ are shown in Figures 1−3; bond lengths and bond angles are collected in the captions.

Because of their propeller shape, $\mathbf{5}^{\cdot}-\mathbf{7}^{\cdot\cdot\cdot}$ are chiral; a few peculiarities of the respective unit cells deserve to be noted. Di(mesityl)([5]trovacenyl)borane ($\mathbf{5}^{\cdot}$) crystallizes in the space group $P\bar{1}$, i.e., the two enantiomorphic forms are crystallographically indistinguishable. (Mesityl)di([5]trovacenyl)borane ($\mathbf{6}^{\cdot\cdot}$) crystallizes in the space group $P2_1$ as a single enantiomer since a mirror plane and a center of symmetry are absent. Finally, $\mathbf{7}^{\cdot\cdot\cdot}$ (space group $P1$) incorporates two independent, chiral molecules in the racemic unit cell.

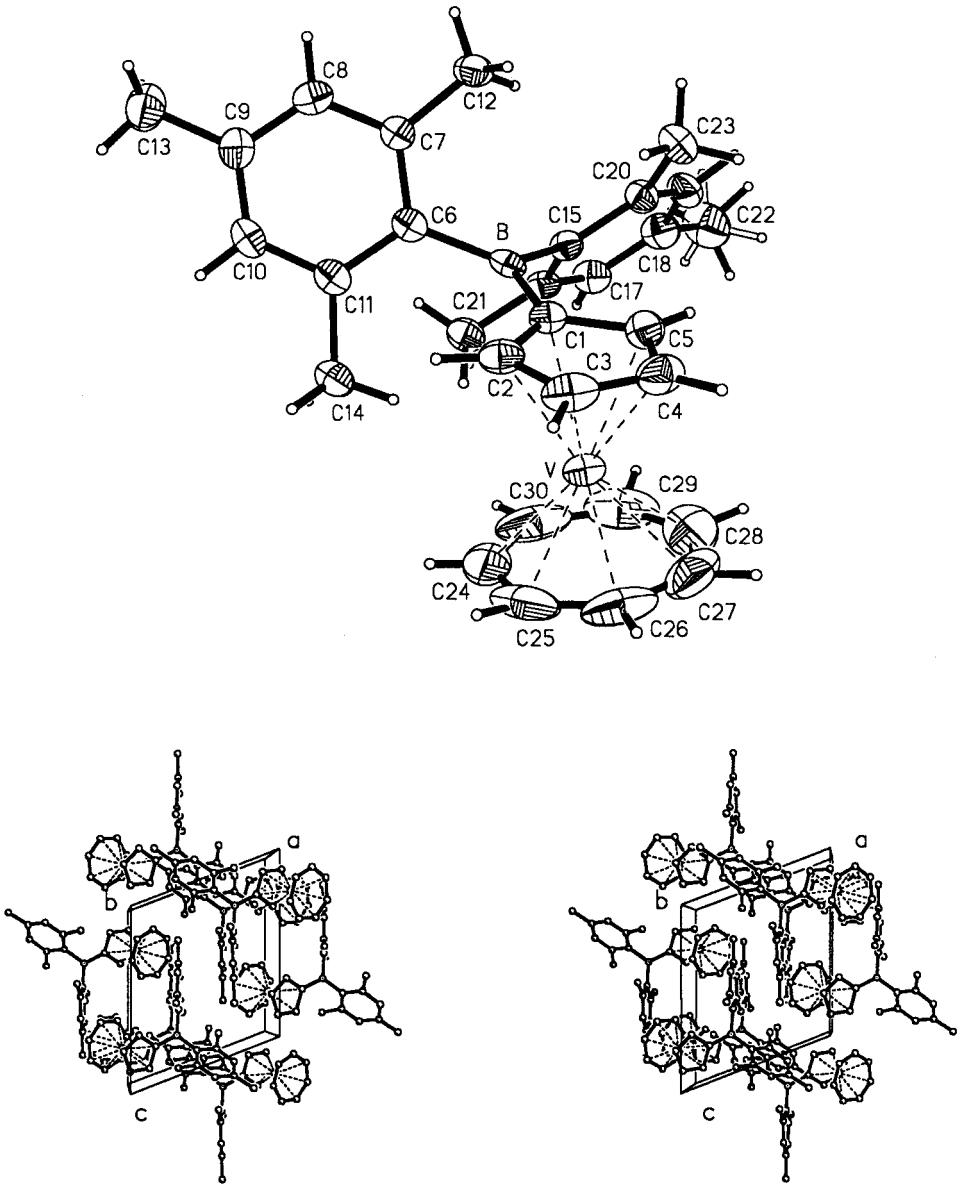


Figure 1. Molecular structure and numbering scheme of compound $\mathbf{5}^{\cdot}$: (top) SHELXTL/LP drawing with 50% probability ellipsoids; (bottom) stereoplot; selected bond lengths (pm) and bond angles (°): B−C1 155.4 (3), B−C6 160.2 (3), B−C15 159.5 (3), C−C ($\eta^5$-Cp, mean value) 141.9, C−C ($\eta^7$-Tr, mean value) 138.6, V−C (Cp, mean value) 226.7, V−C (Tr, mean value) 217.3, V−Cp (centroid) 192.0 (1), V−Tr (centroid) 147.4 (1), C1−B−C6 119.37 (19), C1−B−C15 119.20 (2), C6−B−C15 121.25 (19); important dihedral angles are collected in Table 1

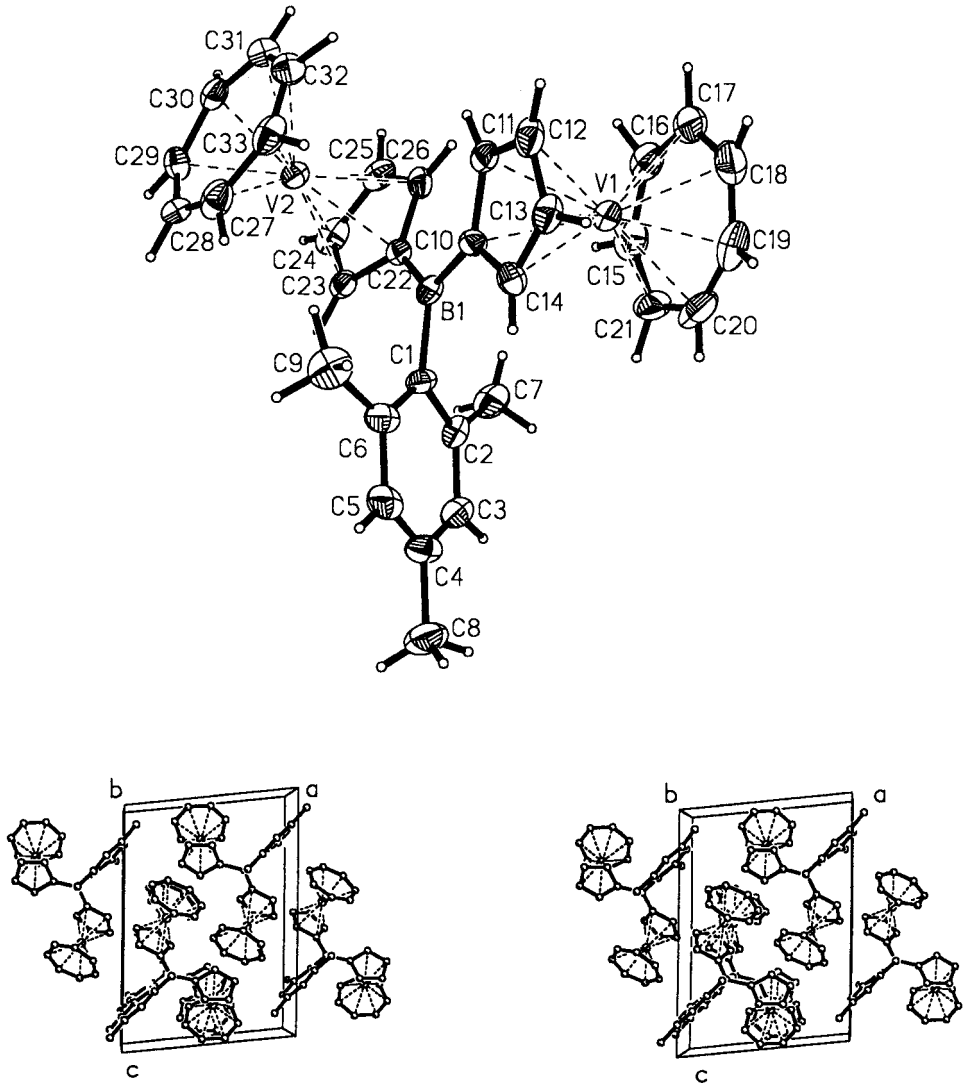


Figure 2. Molecular structure and numbering scheme of compound **6**¨: (top) SHELXTL/LP drawing with 50% probability ellipsoids; (bottom) stereoplot; selected bond lengths (pm) and bond angles (°): B−C1 158.4 (9), B−C10 154.9 (9), B−C22 155.4 (9), C−C ($\eta^5$−Cp, mean value) 142.3, C−C ($\eta^7$-Tr, mean value) 140.4, V−C (Cp, mean value) 226.1, V−C (Tr, mean value) 218.5, V−Cp (centroid) 191.0 (3), V−Tr (centroid) 146.9 (1), C1−B−C10 117.5 (5), C1−B−C22 119.2 (5), C10−B−C22 123.2 (5). V1···V2 589.3; important dihedral angles are collected in Table 1

The following remarks focus on those structural features that may be relevant to the extent of intramolecular communication between the sandwich moieties. The B−$C_{ipso}$ bond lengths involving the organometallic (156 pm) and organic (159 pm) substituents at boron (mean values) differ only marginally. More important are the dihedral angles between the $\eta^5$-cyclopentadienyl and the aryl- and B($C_{ipso}$)$_3$ reference planes PR1, listed in Table 1. The twist of the mesityl plane, with regard to PR1, always surpasses that of the Cp planes. Furthermore, the dihedral angles between the planes Cp and PR1 differ considerably, encompassing the range 4.1−41.7°. This contrasts markedly with the structures of tri(ferrocenyl)borane (**8**), for which these angles lie in the narrow range of 25.8−28.1°[7c] and those of triarylboranes (45−55°[11]). In the context of intersandwich conjugation, the dihedral angles between the cyclopentadienyl planes of the trovacene units connected to boron are of interest: they amount to 25.6° for **6**¨ and to 20.8, 27.3, and 48.1° in the case of **7**‴. However, the torsional angles may be different in fluid solution. Finally, within the error limits, the bond angles about boron add up to 360°, although individual angles differ from 120° (maximal deviation 3°). Consequently, the boron atom is only slightly displaced from the plane defined by the three carbon atoms (3.3 pm for **5**˙; 1.3 pm for **6**¨; 6.6, 4.5 pm for **7**‴).

## Electrochemical Properties

Cyclovoltammetric traces for compounds **5**˙−**7**‴ are depicted in Figure 4, the pertinent data are collected in Table 2. As for the parent complex **4**˙, the trovacenyl boranes **5**˙−7‴ each show one reversible oxidation and one reversible reduction step. Assignment of the redox sites, which are

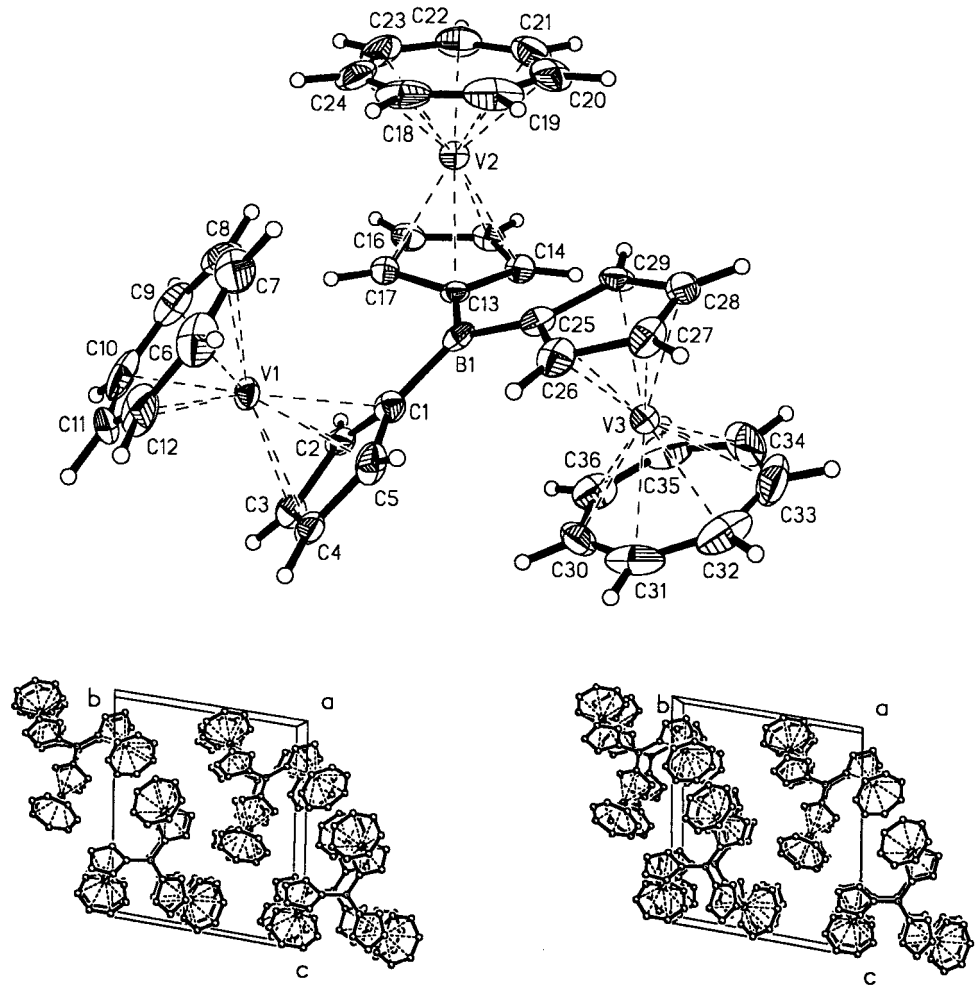


Figure 3. Molecular structure and numbering scheme of compound **7**$^{\cdots}$: (top) SHELXTL/LP drawing with 50% probability ellipsoids; (bottom) stereoplots of the crystallographically independent species **7**$^{\cdots}$ and **7**$^{\cdots}$′; selected bond lengths (pm) and bond angles (°) for **7**$^{\cdots}$: B−C1 156.5 (11), B−C13 157.3 (11), B−C25 156.5 (11), C−C ($\eta^5$-Cp, mean value) 141.6, C−C ($\eta^7$-Tr, mean value) 140.2, V−C (Cp, mean value) 225.5, V−C (Tr, mean value) 217.7, V−Cp (centroid, mean) 190.7 (7), V−Tr (centroid, mean) 146.1 (2), C1−B−C13 117.8 (7), C1−B−C25 122.1 (7), C13−B−C25 119.6 (7). V1···V2 563.0, V2···V3 575.7, V3···V1 609.9; selected bond lengths (pm) and bond angles (°) for **7**$^{\cdots}$′: B′−C1′ 157.3 (11), B′−C13′ 156.3 (11), B′−C25′ 156.2 (11), C′−C′ ($\eta^5$−Cp, mean value) 141.8, C′−C′ ($\mu^7$-Tr, mean value) 140.5, V′−C′ (Cp, mean value) 225.9, V′−C′ (Tr, mean value) 218.2, V′−Cp (centroid, mean value) 190.8 (4), V′−Tr (centroid, mean) 146.1 (2), C1′−B′−C13′ 116.8 (7), C1′−B′−C25′ 120.3 (7), C13′−B′−C25′ 122.7 (6); V1′···V2′ 570.9, V2′···V3′ 585.3, V3′···V1′ 577.0; important dihedral angles are collected in Table 1

responsible for these processes, is based on a comparison with the redox potentials of the components. Thus, the waves at positive potential involve oxidation of the trovacene units. The corresponding potential for the mono(trovacenyl) derivative **5**$^{\cdot}$ underwent a 171 mV anodic shift relative to that of parent **4**$^{\cdot}$, to reflect the electron-accepting properties of the $(Mes)_2B$ substituent.

For the di(trovacenyl) derivative **6**$^{\cdot\cdot}$, a redox splitting $\delta E_{1/2}$-[(2+/+), (+/0)] = 138 mV is clearly resolved, indicating intersandwich communication in **6**$^{\cdot\cdot}$. The value $\delta E_{1/2}$ for **6**$^{\cdot\cdot}$ is very similar to that found for [5−5]di(trovacene) (**10**$^{\cdot\cdot}$) ($\delta E_{1/2}$ = 147 mV[1]), showing that a (Mes)B spacer does not constitute a significant barrier to intramolecular communication between two trovacene units − at least with regard to their mutual influence on the ease of vanadium ionization. Interestingly, the mean value, $[E_{1/2}(2+/+) + E_{1/2}(+/0)]/2$, for dinuclear **6**$^{\cdot\cdot}$ is identical to $E_{1/2}(+/0)$ for mononuclear **5**$^{\cdot}$: primary oxidation of **6**$^{\cdot\cdot}$ is more facile due to the presence of a second, electron-donating trovacene unit; secondary oxidation is less favorable because of the positive charge on **6**$^{+\cdot}$.

Somewhat surprisingly, this behavior is not found for trinuclear **7**$^{\cdots}$ − this complex displays no redox splitting, and despite the presence of three trovacenyl groups, the cathodic shift, relative to the parent, trovacene, is very small. This finding is reminiscent of the redox behavior of molecules containing multiple noninteracting ferrocene units; in this case a CV curve typical for a diffusion-controlled, reversible, one-electron process is obtained ($\Delta E_p$ = 60 mV) where the wave height indicates the number of electrons transferred sequentially.[12] The latter criterion is fulfilled for **7**$^{\cdots}$, since the peak current, relative to the wave at −2.067 V which represents a one-electron process (vide infra), is larger by a factor of three. For **5**$^{\cdot}$ this peak−current ratio (cathodic process: anodic process) is 1:1, for **6**$^{\cdot\cdot}$ it is approximately 1:(1 + 1).

Table 1. Dihedral angles (°) between the reference plane PR1 = $B(C_{ipso})_3$, the planes of the mesityl substituents (Mes), and those of the cyclopentadienyl rings (Cp) of **5**$^{\cdot}$, **6**$^{\cdot\cdot}$, **7**$^{\cdot\cdot\cdot}$ and **7**$^{\cdot\cdot\cdot\prime}$

| | Carbon atoms | Ring plane | PR1 | P2 | P3 |
|---|---|---|---|---|---|
| | 1−5 | P2 (Cp) | 18.56(14) | | |
| **5**$^{\cdot}$ | 6−11 | P3 (Mes) | 63.54(12) | 64.19(13) | |
| | 15−20 | P4 (Mes) | 67.06(13) | 53.16(14) | 72.11(12) |
| | 10−14 | P2 (Cp) | 4.7(4) | | |
| **6**$^{\cdot\cdot}$ | 22−26 | P3 (Cp) | 22.1(4) | 25.6(4) | |
| | 1−6 | P4 (Mes) | 59.0(3) | 55.8(4) | 73.4(4) |
| | 1−5 | P2 (Cp) | 15.7(4) | | |
| **7**$^{\cdot\cdot\cdot}$ | 13−17 | P3 (Cp) | 34.6(4) | 48.1(4) | |
| | 25−29 | P4 (Cp) | 14.3(4) | 27.3(5) | 20.8(4) |
| | 1−5 | P2′ (Cp) | 41.7(4) | | |
| **7**$^{\cdot\cdot\cdot\prime}$ | 13−17 | P3′ (Cp) | 4.1(4) | 41.3(5) | |
| | 25−29 | P4′ (Cp) | 12.6(4) | 29.3(5) | 13.2(5) |

Table 2. Cyclovoltammetric data for the [5]trovacenyl boranes **5**$^{\cdot}$−**7**$^{\cdot\cdot\cdot}$ and for the parent trovacene **4**$^{\cdot}$

| | **4**[a] | **5**[b] | **6**[a] | **7**[a] |
|---|---|---|---|---|
| $E_{1/2}(+/0)$ [V] | 0.260 | 0.431 | 0.362 | − |
| $\Delta E_p$ [mV][b] | 64 | 62 | 64 | |
| $r$[c] | 1 | 1 | 1 | |
| $E_{1/2}(2+/+)$ [V] | − | − | 0.500 | − |
| $\Delta E_p$ [mV][b] | | | 63 | |
| $r$[c] | | | 1 | |
| $E_{1/2}(3+/0)$ [V] | − | − | − | 0.213 |
| $\Delta E_p$ [mV][b] | | | | 56 |
| $r$[c] | | | | ≈1 |
| $\delta E_{1/2}$ [mV][d] | − | − | 138 | n.r. |
| $E_{pa,1}$ [V][a] | − | 1.02 | 1.16 | 0.96 |
| $E_{pa,2}$ [V][a] | | 1.12 | | |
| $E_{1/2}(0/-)$ [V] | −2.550 | −2.067 | −2.095 | −2.067 |
| $\Delta E_p$ [mV][b] | 66 | 62 | 70 | 58 |
| $r$[c] | 1 | 1 | 1 | 0.9 |
| $E_{pc,1}$ [V][c] | − | − | − | −2.7 |

[a] In 1,2-dimethoxyethane/0.1 M tetraethylammonium perchlorate at a glassy carbon electrode versus a saturated calomel electrode. − [b] $\Delta E_p = (E_{pa} - E_{pc})$. − [c] $r = I_{pa}/I_{pc}$. − [d] $\delta E_{1/2} = E_{1/2}(2+.+) - E_{1/2}(+/0)$.

Why, within the framework of the CV experiment, do the trovacene units appear to be interacting in **6**$^{\cdot\cdot}$ but noninteracting in **7**$^{\cdot\cdot\cdot}$? If one assumes that trovacenyl groups are sterically more demanding than mesityl groups, it is conceivable that, in fluid solution, the twisting of the trovacene units relative to the $BC_3$ reference plane is more extensive in **7**$^{\cdot\cdot\cdot}$ than in **6**$^{\cdot\cdot}$. Since, arguably, an intersandwich interaction requires conjugation, a large twist distortion in **7**$^{\cdot\cdot\cdot}$ would explain the absence of an observable redox splitting. In this context it is worth mentioning that the solid-state and fluid-solution structures of the related molecule tri(ferrocenyl)borane (**8**) were found to be disparate,[7c] in the fluid solution, one ferrocenyl group is oriented opposite to the other two with respect to the central $BC_3$ plane. Since its electrochemical data were unavailable, we resynthesized **8** and recorded its cyclovoltammogram. As for **7**$^{\cdot\cdot\cdot}$, no redox splitting is resolved for **8** and, relative to ferrocene [$E_{1/2}(+/0)$ = 0.49 V], the potential $E_{1/2}(+/0)$ = 0.42 V for **8** represents a small cathodic shift.

In the strongly cathodic region of the potential, **5**$^{\cdot}$−**7**$^{\cdot\cdot\cdot}$ give rise to waves which signalize one-electron processes. This is inferred when their peak currents are compared to those representing the oxidation of the trovacene groups (vide supra). Furthermore, the numerical values of the potentials $E_{1/2}$ = −2.067 (**5**$^{\cdot}$), −2.095 (**6**$^{\cdot\cdot}$), −2.067 V (**7**$^{\cdot\cdot\cdot}$) are closer to $E_{1/2}(0/-)$ = −1.94 V[10] of 1,3,5-tri(mesityl)borane (**9**), than that of trovacene(**4**) [$E_{1/2}(0/-)$ = −2.55 V]. The cathodic shift observed for **5**$^{\cdot}$ (0/−), **6**$^{\cdot\cdot}$ (0/−) and **7**$^{\cdot\cdot\cdot}$ (0/−) relative to **9** (0/−) reflects the superior electron-donating properties of trovacenyl versus mesityl. Reduction of trovacenylboranes therefore must be regarded as boron-centered. Subsequent vanadium-centered reductions of the [5]trovacenylborane anions **5**$^{-}$−**7**$^{-}$ probably lie close to or outside the electrochemical window, i.e., at potentials < −2.9 V.

## EPR Spectroscopy and Magnetic Susceptibility

The availability of the mono-, di-, and tri([5]trovacenyl)boranes **5**$^{\cdot}$−**7**$^{\cdot\cdot\cdot}$ permits a systematic study of the substituent effect of an $R_2B$ group, as well as of the relative mediating properties of the RB< and −B< units. EPR spectra of **5**$^{\cdot}$−**7**$^{\cdot\cdot\cdot}$ are shown in Figures 5−7, the parameters, confirmed by simulation, are collected in Table 3.

The most remarkable feature in the fluid-solution spectrum of di(mesityl)([5]trovacenyl)borane (**5**$^{\cdot}$) is the fairly large coupling constant $a(^{51}V)$ = −7.35 mT, which exceeds the value for parent **4**$^{\cdot}$ by 6%. As for phenyl([5]trovacene),[1] this increase can be rationalized by a π-electron donation [$\eta^5$-$C_5H_4(e_2) \rightarrow B(sp^2)$] which raises the positive partial charge on the central vanadium atom with concomitant V{3d($z^2$)} orbital contraction. This will have the effect of decreasing V{3d($z^2$)}/ligand($a_1$) overlap, thereby diminishing metal → ligand spin delocalization and slightly raising the coupling constant $a(^{51}V)$. The electronic perturbation of the trovacene unit by the dimesitylboryl substituent is insufficient, however, to effect an observable change of the $g$ tensor from axial (**4**$^{\cdot}$) to orthorhombic (**5**$^{\cdot}$) which would be required by symmetry.

(Mesityl)di([5]trovacenyl)borane (**6**$^{\cdot\cdot}$) in fluid solution gives rise to a typical diradical EPR spectrum; the 15-line hyperfine pattern approaches a binomial intensity distribution with splitting that amounts to half the value of a ($^{51}V$) for the monoradical **5**$^{\cdot}$. Spectral simulation furnished optimal agreement for the exchange coupling constant $J_{EPR}$ = |1.43| $cm^{-1}$ which represents half the magnitude of $J$ obtained for [5−5]di(trovacene) (**10**$^{\cdot\cdot}$).[1] In conditions close to the "fast-exchange limit", however, two caveats are called for: (1) spectral simulation does not provide the sign for $J$ (magnetic susceptibility suggests that $J$ < 0, vide infra), and (2) not too much confidence should be placed on the numerical value of $J$ in this situation. Yet, the qualitative conclusion, that the incorporation of an −(R)B− spacer

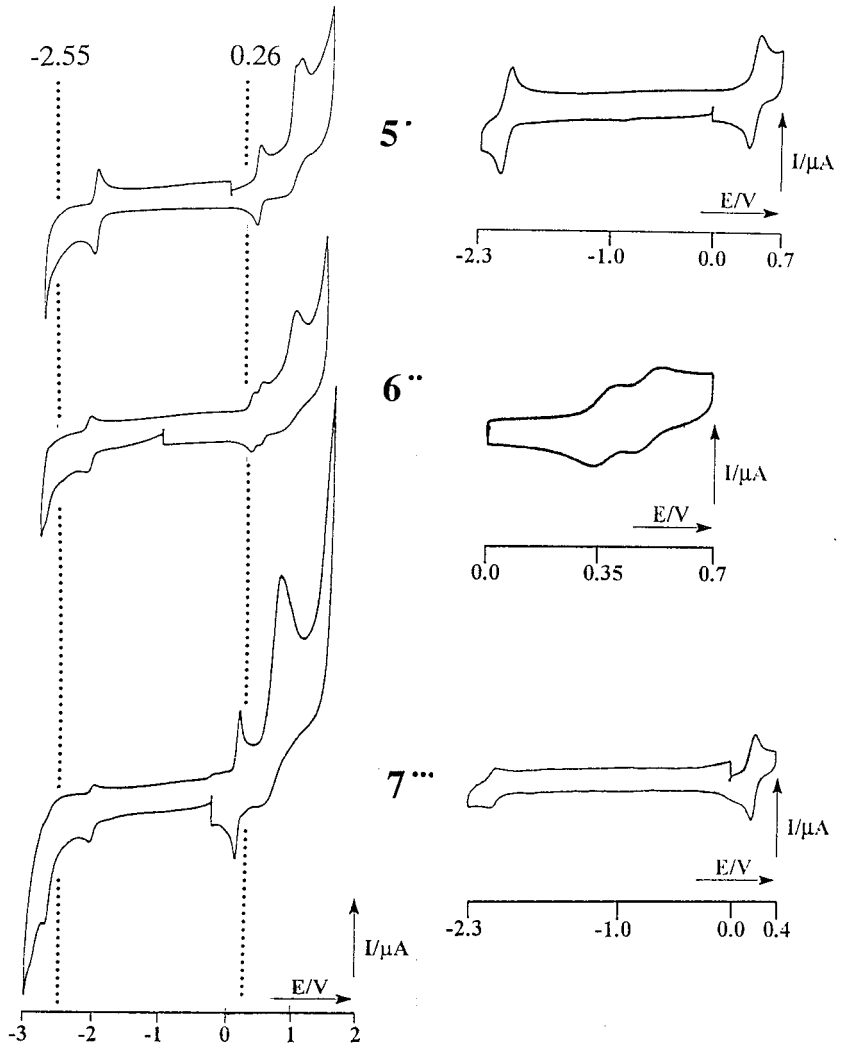


Figure 4. Cyclic voltammetric traces for compounds $\mathbf{5}^{\cdot}-\mathbf{7}^{\cdot\cdot\cdot}$ (1,2-dimethoxyethane/0.1 M tetrabutylammonium perchlorate, at glassy carbon versus SCE, $v = 100$ mV $s^{-1}$, −40 °C); the dotted lines mark the potentials for the processes $\mathbf{4}^{\cdot}$ (+/0) and $\mathbf{4}^{\cdot}$ (0/−) of the parent trovacene

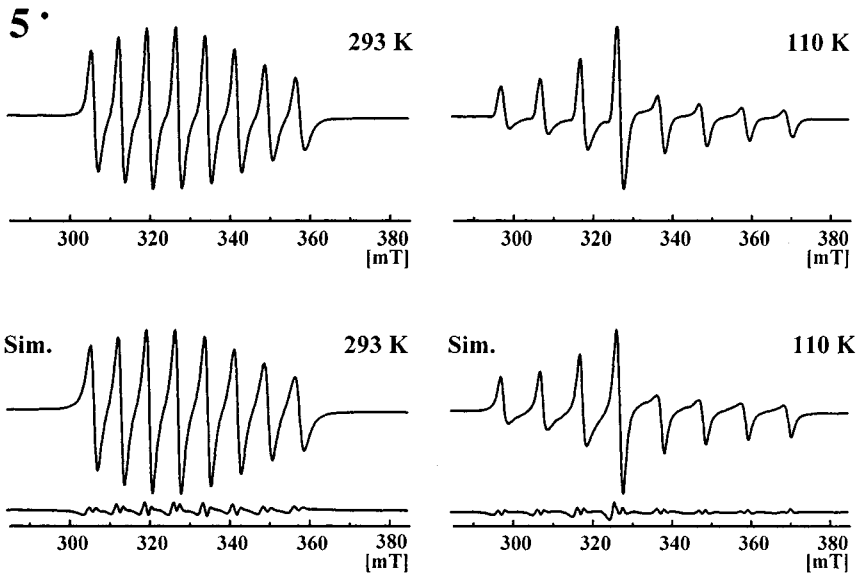


Figure 5. EPR spectra (X-band) of $\mathbf{5}^{\cdot}$, fluid (293 K) and rigid (110 K) solution in toluene, with simulated traces (bottom)

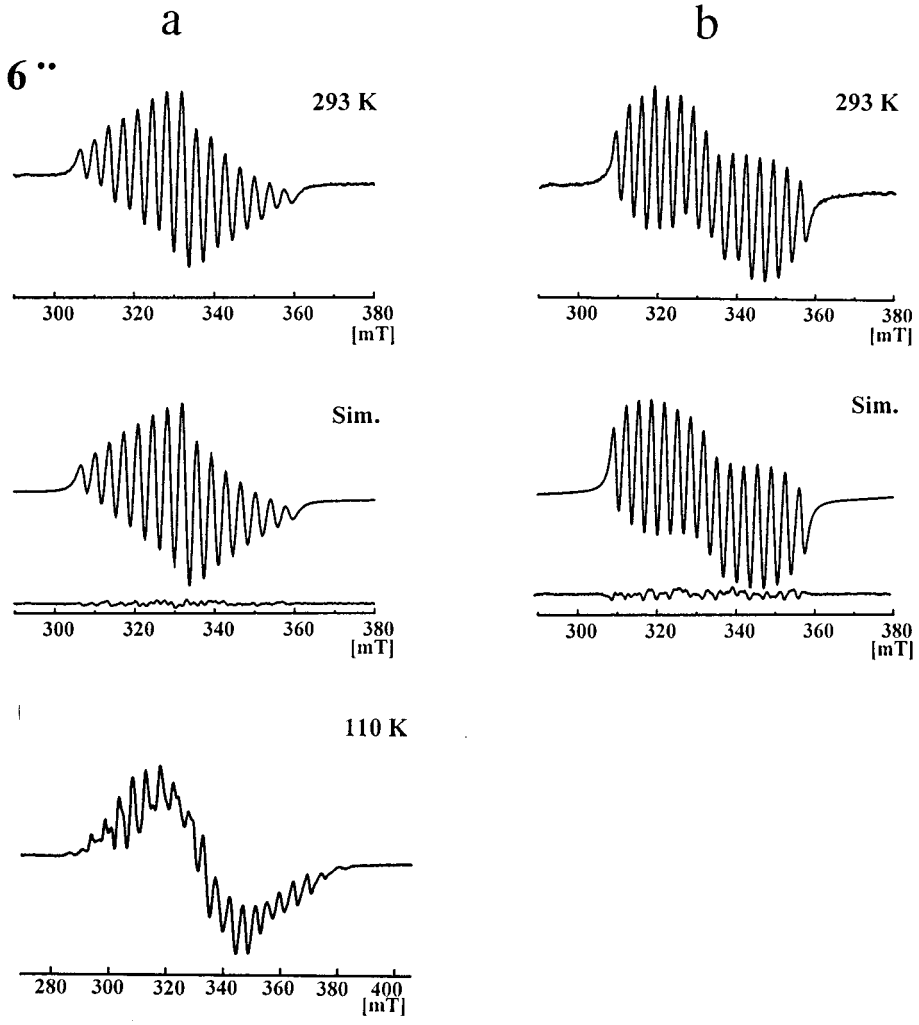


Figure 6. EPR spectra (X-band) of **6**··, fluid (293 K) and rigid (110 K) solution in THF (a), and spectra obtained after addition of *n*-butyllithium in hexane (b)

between two [5]trovacenyl units attenuates exchange coupling to a small degree only, is warranted. If conjugation between the $\eta^5$-$C_5H_4$ π-perimeters and the vacant B($2p_z$) orbital contributes to the exchange interaction, this result does not come as a surprise, since for **6**·· the dihedral angles between the ligand- and reference planes are small in the crystal structure (Table 1) and, due to conformational mobility, they are variable in fluid solution. However, as in the case of [5−5]di(trovacene),[1] the detailed coupling path between the two V($d^5$) centers is not clear. Overlap of the V{3d($z^2$)} orbitals, which dominate the SOMOs of the trovacene units, with the σ-backbone of the μ[$\eta^5$:$\eta^5$-$C_5H_4B(Mes)C_5H_4$] bridge, is small, as demonstrated by the small hyperfine coupling constant $a(^1H_{Cp})$ = 0.18 mT in the EPR spectrum of **4**·. Therefore, the direct coupling mechanism and the indirect one, which operates by polarization of filled π-orbitals of the ligands by the singly occupied V{3d($z^2$)} orbitals, may be of comparable magnitude. Both mechanisms are of low efficiency, though, and the resulting type of interaction − ferromagnetic or antiferromagnetic − is difficult to predict.

Information concerning the spin-exchange path between the two vanadium centers was also expected from the influence that coordination of a Lewis base to boron would exert on the EPR spectrum of **6**··. The EPR trace for **6**·· in the presence of *n*-butyllithium is shown in Figure 6, where the spectral parameters, verified by computer simulation, are also given. Formation of the adduct [**6**··−*n*Bu]$^-$ clearly affects the EPR spectrum, from which the reduced value $J_{EPR}$ = |0.97| $cm^{-1}$ for the exchange coupling constant can be derived by simulation. No discernible change is observed on the addition of triethylamine, indicating that, probably due to steric hindrance, no adduct formation occurs. Exchange interaction is attenuated in [**6**··−*n*Bu]$^-$, presumably because the exchange path is modified in two ways: (1) The vacant boron $p_z$ orbital, which potentially may engage in conjugative interactions between the trovacenyl units, is transformed into an orbital used for σ-bonding to the Lewis base, and (2) The boron atom is rehybridized from $sp^2$ to $sp^3$ during the process **6**·· → [**6**··−*n*Bu]$^-$. Both effects, elimination of a vacant p-orbital in the bridge and decrease of the B(2s) content in the σ-orbitals radiating from boron

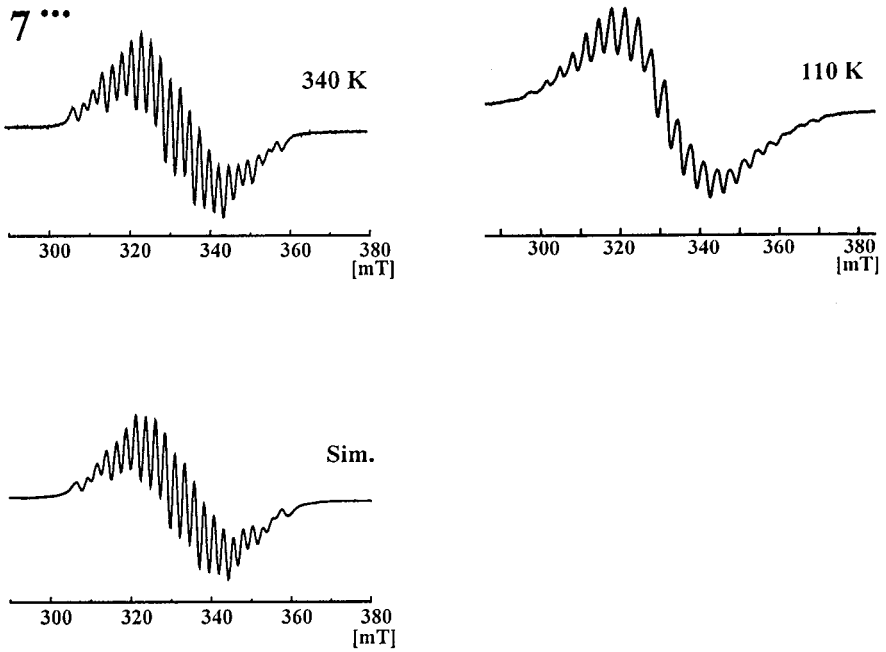


Figure 7. EPR spectra (X-band) of $\mathbf{7}^{\cdot\cdot\cdot}$, fluid (340 K) and rigid (110 K) solution in toluene, with the simulated trace (bottom)

Table 3. EPR data for the trovacenyl boranes $\mathbf{5}^{\cdot}$, $\mathbf{6}^{\cdot\cdot}$, and $\mathbf{7}^{\cdot\cdot\cdot}$, trovacenylborate $[\mathbf{6}^{\cdot\cdot}-n\mathrm{Bu}]^-$, and trovacene $\mathbf{4}^{[a]}$

| | $\mathbf{4}^{\cdot}$ | $\mathbf{5}^{\cdot}$ | $\mathbf{6}^{\cdot\cdot}$ | $\mathbf{7}^{\cdot\cdot\cdot}$ | $[\mathbf{6}^{\cdot\cdot}-n\mathrm{Bu}]^-$ |
|---|---|---|---|---|---|
| $g_{iso}$ | 1.9866 | 1.9789 | 1.9785 | 1.978 | 1.9788 |
| $a(^{51}\mathrm{V})$ [mT] | −6.98 | −7.35 | −7.32 | −7.24 | −6.69 |
| $\lvert J\rvert$ [cm$^{-1}$] | – | – | \|1.43\| | \|0.5\| | \|0.97\| |
| $g_{\parallel}$ | 2.0030 | 1.9970 | – | – | – |
| $g_{\perp}$ | 1.9784 | 1.9688 | – | – | – |
| $A_{\parallel}$ ($^{51}$V) [mT] | −1.39 | −1.27 | – | – | – |
| $A_{\perp}$ ($^{51}$V) [mt] | −9.61 | −10.35 | – | – | – |

[a] $^{m}_{I}$ ($^{51}$V)-dependent line width effects were included in the simulations.

may contribute to the observed reduction in exchange coupling, but apportioning their relative contributions is unfeasible. The gradation in $J$ values of the diradicals containing B(sp$^2$) or B(sp$^3$) atoms in the spacer is an empirical observation which, for a detailed analysis, must await additional evidence. It is noteworthy, however, that a similar trend is encountered in the $^1$H NMR spectra of boranes, in that nuclear spin coupling across boron is weakened if boranes $R_3B$ are converted into borates $[R_3BR']^-$.[13]

Additional interesting aspects are offered by tri([5]trovacenyl)borane $\mathbf{7}^{\cdot\cdot\cdot}$. Whereas numerous organic triradicals have been prepared and studied in great detail,[14] and inorganic species possessing three paramagnetic centers are also familiar,[15] very few organometallic triradials have been reported so far.[16] This is surprising, since the choice of open-shell metal atoms whose nuclei bear magnetic moments suitable for EPR study, and the almost unlimited variability of organic frameworks serving as potential spacers, should provide a rich playground for investigation. Further assets of organometallic oligoradicals include the feasability of EPR studies in fluid solution (most organometallics contain mainly covalent bonds that suppress dissociation in solution), as well as their attenuated reactivity, compared to that of organic radicals. The synthesis and characterization of organometallic oligoradicals is interesting both from a fundamental point of view (study of competing interactions and spin frustration) as well as from an applied perspective (generation of high-spin molecules with ferromagnetic properties).

The fluid-solution EPR spectrum of tri([5]trovacenyl)borane $\mathbf{7}^{\cdot\cdot\cdot}$ exhibits a 22-line multiplet whose $^{51}$V splitting corresponds to one third of the hyperfine coupling for mononuclear trovacene $\mathbf{4}^{\cdot}$ (Figure 7). The intensity distribution and the line shapes deviate markedly from the simple binomial case (fast-exchange limit) so that deriving the parameter $J$ by computer simulation appears practicable. The numerical value $J = |0.53|$ cm$^{-1}$ thus obtained for the exchange interaction in $\mathbf{7}^{\cdot\cdot\cdot}$ is somewhat unreliable, though, because it exceeds the coupling constant $a(^{51}\mathrm{V})$ by a factor of 100 which means that the fast-exchange limit is very close. A comparison of the exchange interactions of $\mathbf{6}^{\cdot\cdot}$, $\mathbf{7}^{\cdot\cdot\cdot}$, and $\mathbf{10}^{\cdot\cdot}$ will therefore be based on $J$ values gathered from magnetic susceptibility studies.

Magnetic susceptibilities of crystalline powders of diradical $\mathbf{6}^{\cdot\cdot}$ and triradical $\mathbf{7}^{\cdot\cdot\cdot}$ were measured on a SQUID magnetometer in the temperature range 1.8−250 K and at constant magnetic fields of 500 and 5000 G. Plots of the dependence of the inverse susceptibility, $\chi^{-1}$, vs temperature, T, for both radicals are shown in Figure 8.

The Bleaney−Bowers type equation, Equation 1[15d] was fitted to the experimental data of the diradical $\mathbf{6}^{\cdot\cdot}$ (Figure 8a) to give the best-fit parameters for the factor $g = 1.99(1)$, the exchange constant $J/k = -1.38(2)$ K ($-0.96$ cm$^{-1}$) and the Curie−Weiss temperature $\Theta = -9.5(5)$ K. Therefore, the interaction in $\mathbf{6}^{\cdot\cdot}$ is antiferromagnetic.

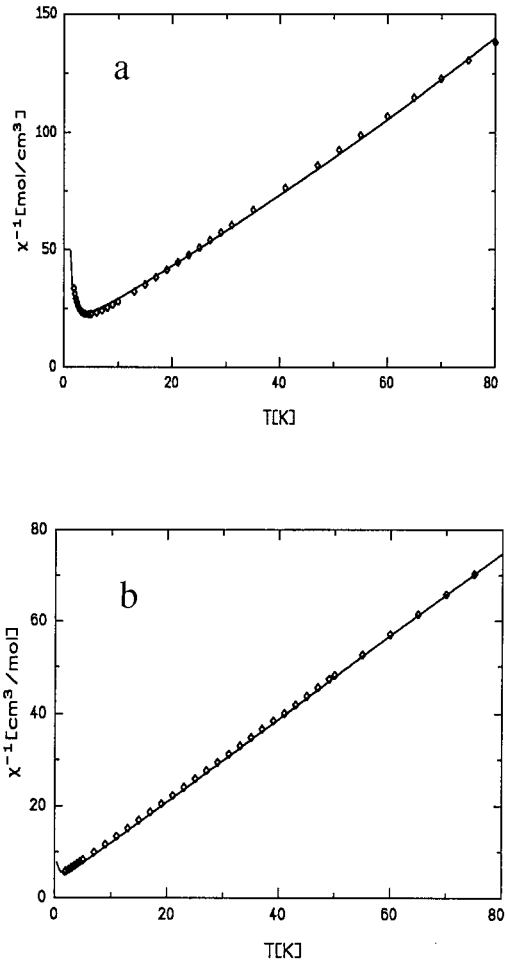


Figure 8. Temperature-dependence of the inverse molar susceptibility of the diradical **6**·· and the triradical **7**···

$$\chi_{mol} = \frac{2N g^2 \mu_B^2}{kT[3+\exp(-J/kT)]} \quad \frac{T}{(T-\Theta)} \qquad (1)$$

This is also the case for triradical **7**··· whose susceptibility data (Figure 8b) were fitted by Equation 2, which applies to the case of an equilateral triangular disposition of identical $S = 1/2$ centers.[17] Optimal fit of the curve was obtained by means of the parameters $g = 1.99(1)$, $J/k = -0.5(2)$ K ($-0.35$ cm$^{-1}$), $\Theta = -2.7(5)$ K. From an inspection of the least-squares fit in Figure 8b one has to conclude that the derived exchange constant $J$ can only be interpreted as an upper limit of the interaction parameter. If the local spins present in **7**··· are denoted as $S_1$, $S_2$, and $S_3$, the spin Hamiltonian describing the low-lying states in zero field may be expressed as Equation 3.

$$\chi_{mol} = \frac{N g^2 \mu_B^2}{2kT} \quad \frac{1+5\exp(-3J/kT)}{1+\exp(-3J/kT)} \quad \frac{T}{(T-\Theta)} \qquad (2)$$

$$H = -2J(S_1S_2+S_1S_3+S_2S_3) \qquad (3)$$

The interaction between the three local doublets leads to a molecular quartet and two degenerate doublets, the latter forming the ground state as implied by the antiferromagnetic nature of the interaction. Here, the separation between the degenerate doublets and the quartet amounts to 3*J*. The analysis of the susceptibility data reveals that $J$(**7**···) for the triradical falls considerably short of $J$(**6**··) obtained for the diradical. The same gradation was found for the EPR spectra of **7**··· and **6**··. This finding reflects the spin frustration in **7**··· where three spins $S = 1/2$ that are coupled antiferromagnetically, reside in an equilateral triangular arrangement (Figure 3, Figure 9). The reduced $J$ value results because, in the doublet ground state of **7**···, two spins need to be aligned parallel, the opposite of the tendency towards spin pairing (as demonstrated by the susceptibility curve for diradical **6**··).

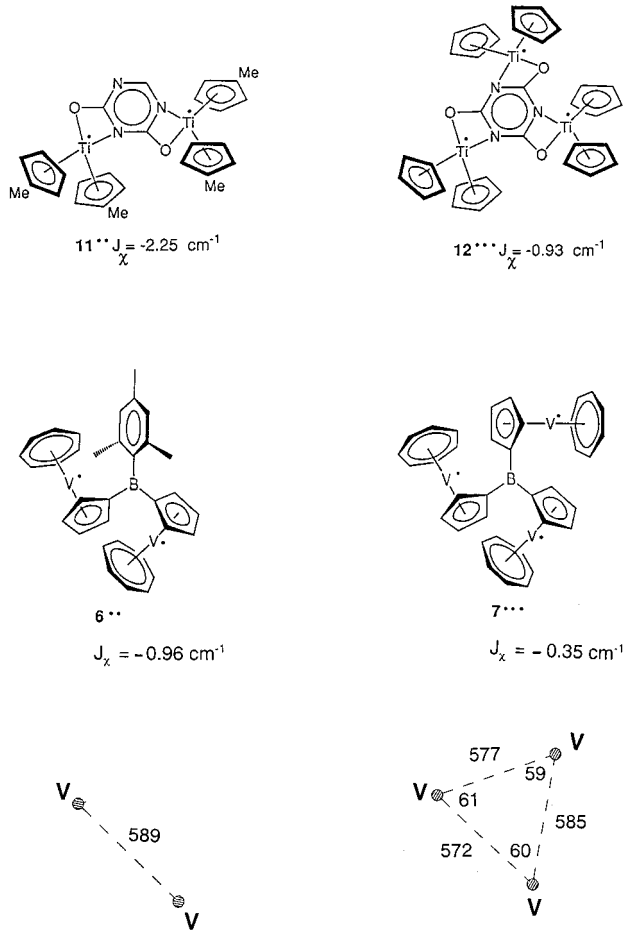


Figure 9. Structures of the organometallic diradicals/triradicals 11··/12··· and 6··/7···, and their exchange coupling constants $J_{\χ}$; intervanadium distances (pm) in 6·· and 7··· are also given

The characteristic decrease in the magnitude of $J$ on going from a diradical to a triradical of triangular structure, while keeping the exchange path identical, is limited to cases where the pairwise interactions are antiferromagnetic. Organic triradicals with the requisite trigonal symmetry are usually based on 1,3,5-benzenetriyl as backbone, where the 1,3-connection effects ferromagnetic coupling.[18] Therefore, to the best of our knowledge, spin frustration has as yet only been observed once for an organic triradical.[14d] In

contrast, several examples of spin-frustrated coordination compounds[19] are known, and there are also a few cases known in the field of organometallic chemistry.[20,5a] Since the pair **11**$^{\cdot\cdot}$/**12**$^{\cdot\cdot\cdot}$[20] resembles the pair **6**$^{\cdot\cdot}$/**7**$^{\cdot\cdot\cdot}$ reported here, they are represented in Figure 9 together with their respective *J* values, determined by susceptometry. What both pairs have in common is the presence of two or three paramagnetic sandwich complex units ($S = 1/2$) whose open-shell central metal atoms, Ti($d^1$) or V($d^5$), are linked by bridges which effect antiferromagnetic coupling. Furthermore, in the trinuclear complexes **7**$^{\cdot\cdot\cdot}$ and **12**$^{\cdot\cdot\cdot}$, the central metal atoms are placed at the corners of an equilateral triangle so that the pairwise magnetic interactions are governed by a single exchange parameter *J*. Thus, the stage is set for spin frustration which is actually observed in both cases since, despite identical coupling paths, *J* for the triradicals **7**$^{\cdot\cdot\cdot}$ and **12**$^{\cdot\cdot\cdot}$ falls short of *J* exhibited by diradicals **6**$^{\cdot\cdot}$ and **11**$^{\cdot\cdot}$. It may come as a surprise that the *J* values for **11**$^{\cdot\cdot}$ and **12**$^{\cdot\cdot\cdot}$ exceed those for **6**$^{\cdot\cdot}$ and **7**$^{\cdot\cdot\cdot}$ considerably, despite the fact that, in both cases, the interacting metal atoms are separated by four bonds. One should bear in mind, however, that a detailed description of the exchange pathway must be based on the symmetry relationship between the metal- and ligand bridge orbitals and their energies. The two systems compared here differ significantly in that the singly occupied titanium orbitals in **11**$^{\cdot\cdot}$ and **12**$^{\cdot\cdot\cdot}$ are thought to be located in the plane of the bridging cyanurato trianion,[20] whereas in the [5]trovacenyl derivatives **6**$^{\cdot\cdot}$ and **7**$^{\cdot\cdot\cdot}$, the singly occupied vanadium orbitals are perpendicular to the cyclopentadienyl plane of the $\mu[\eta^5{:}\eta^5\text{-}C_5H_4B(R)C_5H_4]$ bridge (R = mesityl, trovacenyl). A simple count of the atoms intervening between the two paramagnetic centers can therefore not account for the gradation of the experimental *J* values.

## Experimental Section

**General:** All manipulations were performed with exclusion of air under dinitrogen or argon (CV) unless stated otherwise. Physical measurements were carried out with equipment specified previously.[22] Trovacene $(\eta^7\text{-}C_7H_7)V(\eta^5\text{-}C_5H_5)$,[6a] di(mesityl)fluoroborane, and (mesityl)difluoroborane[23] were prepared as described in the literature.

**Bis(mesityl)([5]trovacenyl)borane (5$^{\cdot}$):** To a solution of trovacene (290 mg, 1.4 mmol) in 80 mL of diethyl ether was added, at room temperature, 1.4 mL of a solution of *n*-butyllithium in hexane (1.55 mol $L^{-1}$). After being stirred for 14 h, the reddish-brown solution was cooled to −40 °C, and 187 mg (0.7 mmol) of di(mesityl)fluoroborane, dissolved in 30 mL of diethyl ether, was slowly added to it. The mixture was allowed to reach room temperature, whereby a color change to green occurred. After the reaction mixture was stirred for 20 h, the solvent was removed in vacuo, the residue was taken up in toluene and subjected to column chromatography ($Al_2O_3$, 0% $H_2O$, elution with toluene). From the first fraction, 290 mg (0.65 mmol, yield: 46%) of **5**$^{\cdot}$ was obtained as a green product. Single crystals suitable for X-ray diffraction were grown from benzene/*n*-pentane (supernatant). MS (EI, 70 eV) *m*/*z* (%): 456

Table 4. Crystallographic data for the compounds **5**$^{\cdot}$, **6**$^{\cdot\cdot}$, and **7**$^{\cdot\cdot\cdot}$

| | **5**$^{\cdot}$ | **6**$^{\cdot\cdot}$ | **7**$^{\cdot\cdot\cdot}$ |
|---|---|---|---|
| Shape, color | plates, green | thin plates, dark | prisms, dark red |
| Crystal size (mm) | 0.30 × 0.15 × 0.06 | 0.30 × 0.15 × 0.06 | 0.18 × 0.18 × 0.15 |
| Crystal system | Triclinic | Monoclinic | Triclinic |
| Space group | *P*1bar (No. 2), $Z = 2$ | $P2_1$ (No 12), $Z = 2$ | *P*1 (No. 1), $Z = 2$ |
| Unit cell dimensions | $a = 9.7666(9)$ Å, $\alpha = 91.259(11)°$ | $a = 10.1842(19)$ Å. | $a = 7.796(2)$ Å, $\alpha = 98.94(3)°$ |
| | $b = 11.4985(11)$ Å, | $b = 8.9716(13)$ Å, $\beta = 96.139(9)°$ | $b = 12.429(3)$ Å, $\beta = 94.67(3)°$ |
| | $\beta = 110.611(11)°$, | | |
| | $c = 11.5003(11)$ Å, $\gamma = 94.302(11)°$ | $c = 14.350(2)$ Å | $c = 14.599(6)$ Å, $\gamma = 93.15(2)°$ |
| Volume | 1203.8(2) Å$^3$ | 1303.6(4) Å$^3$ | 1389.5(8) Å$^3$ |
| Empirical formula | $C_{30}H_{33}BV$ | $C_{33}H_{33}BV_2$ | $C_{36}H_{33}BV_3$ |
| Formula mass | 455.31 | 522.28 | 629.25 |
| Density (calculated) | 1.256 Mg/m$^3$ | 1.382 Mg/m$^3$ | 1.504 Mg/m$^3$ |
| Absorption coefficient | 0.427 mm$^{-1}$ | 0.737 mm$^{-1}$ | 1.014 mm$^{-1}$ |
| *F*(000) | 482 | 564 | 646 |
| Diffractometer type | Stoe IPDS | Siemens P4 | Nonius CAD4 |
| Wavelength | 0.71073 Å | 0.71073 Å | 0.71073 Å |
| Temperature | 193(2) K | 223(2) K | 203(2) K |
| θ range for data collection | 2.24 to 25.94° | 2.01 to 25.05° | 2.35 to 26.32° |
| Index ranges | −11/11, −14/14, −12/14 | −1/12, −9/10, −17/17 | −9/9, −15/15, −18/17 |
| Data-collection software | Stoe Expose | Siemens XSCANS | Nonius EXPRESS |
| Cell-refinement software | Stoe Cell | Siemens XSCANS | Nonius EXPRESS |
| Data-reduction software | Stoe Integrate | Siemens SHELXTL | XCAD4 (Harms, 1998) |
| Reflections collected | 8561 | 5830 | 7404 |
| Independent reflections | 4352 [$R$(int) = 0.0617] | 4118 [$R$(int) = 0.0615] | 7404 |
| Observed reflections | 2930 [$I > 2\sigma(I)$] | 3041 [$I > 2\sigma(I)$] | 5889 [$I > 2\sigma(I)$] |
| Reflections used for refinement | 4352 | 4118 | 7404 |
| Flack param. (abs. structure) | − | −0.07(4) | 0.37(4) (racemic twin) |
| Largest diff. peak and hole | 0.342 and −0.316 e·Å$^{-3}$ | 0.315 and −0.341 e·Å$^{-3}$ | 0.497 and −0.511 e·Å$^{-3}$ |
| Data/restraints/parameters | 4352/0/410 | 4118/1/424 | 7404/3/722 |
| Goodness-of-fit on $F^2$ | 0.903 | 1.082 | 1.035 |
| *R* index (all data) | *wR*2 = 0.0930 | *wR*2 = 0.1067 | *wR*2 = 0.1277 |
| *R* index conventional [$I > 2\sigma(I)$] | *R*1 = 0.0419 | *R*1 = 0.0532 | *R*1 = 0.0559 |

(34.8), 455 (100) [$M^+$], 454 (27), 364 (43.5) [$M^+ - C_7H_7$]. − IR (KBr): $\tilde{\nu}$ = 3029 $cm^{-1}$ (w), 2912 (m), 1800−1600 (w), 1605 (m), 1436 (s), 1363 (s), 1251 (m), 798 (s), 782 (s), 470 (w), 432 (w). − Voltammetry and EPR: see text. − $C_{30}H_{33}BV$ (455.34): calcd. C 79.13, H 7.30; found C 78.06, H 7.43.

**Mesityldi([5]trovacenyl)borane (6¨):** For the preparation of **6¨**, the instructions given for **5˙** were followed with: 342 mg (1.65 mmol) of trovacene dissolved in 90 mL of diethyl ether, 1.7 mL of *n*-butyllithium (1.55 mol $L^{-1}$ in *n*-hexane), and 68 mg (0.4 mmol) of (mesityl)difluoroborane in 30 mL of diethyl ether. Column chromatography delivered **6¨** in the second fraction as a green material, yield: 170 mg (0.31 mmol, 38%). Crystals were obtained by slow evaporation of a solution of **6¨** in toluene. MS(EI, 70 eV) *m*/*z* (%): 543 (25.5), 542 (100) [$M^+$], 541 (8), 271 (17) [$M^{2+}$]. − IR (KBr): $\tilde{\nu}$ = 3039 $cm^{-1}$ (w), 2951, 2916 (m), 1750−1600 (w), 1604 (m), 1443 (s), 1363 (s), 1243 (m), 1052 (s), 810, 783 (s), 430 (w). − Voltammetry and EPR: see text. − $C_{33}H_{33}BV_2$ (542.32): calcd. C 73.03, H 6.13; found C 72.47, H 5.67.

**Tri([5]trovacenyl)borane (7‴):** The synthesis proceeded as described for **5˙** and **6¨**; however, the 20 h period of reacting [5]trovacenyllithium with $BF_3{\cdot}OEt_2$ at room temperature was followed by 30 min of refluxing. From trovacene (453 mg, 2.19 mmol), *n*-butyllithium (2.2 mL of a solution 1.55 mol $L^{-1}$ in *n*-hexane), and $BF3{\cdot}Et_2O$ (50 mg, 0.36 mmol), 174 mg (0.28 mmol, yield: 39%) of **7‴** was obtained, which could be recrystallized from benzene/*n*-pentane (supernatant) to form green needles. MS (EI, 70 eV) *m*/*z* (%): 630 (38), 629 (100) [$M^+$], 628 (24), 315 (22) [$M^{2+}$]. − IR (KBr) $\tilde{\nu}$ = 3041 $cm^{-1}$ (w), 2959 (m), 1750−1600 (w), 1434 (m), 1373 (s), 1263 (m), 1058 (s), 802, 782 (s), 426 (w). − Voltammetry and EPR: see text. − $C_{36}H_{33}BV_3$ (629.32): calcd. C 68.71, H 5.29; found C 67.73, H 5.13.

**X-ray Crystal Structure Analyses of 5˙, 6˙, and 7‴:** The crystal structures were solved by direct methods (SHELXS-97) and refined by the full matrix least squares refinement on $F^2$ values (SHELXL-97), all non-hydrogen atoms were refined anisotropically. Hydrogen atoms were included on calculated positions (**6¨**, **7‴**) or were refined isotropically (compound **5˙**). See also Table 4. Further crystallographic data (excluding structure factors) for the structures reported in this paper were deposited with the Cambridge Crystallographic Data Centre as supplementary publication nos. CCDC-132390−132392. Copies of the data may be obtained free of charge on application to CCDC, 12 Union Road, Cambridge CB2 1EZ, UK [Fax: (internat.) +44-1223/336-033; E-mail: deposit@ccdc.cam.ac.uk].

## Acknowledgments

Support of this work by the Volkswagen-Stiftung and the Fonds der Chemischen Industrie is gratefully acknowledged.

[1] C. Elschenbroich, O. Schiemann, O. Burghaus, K. Harms, J. Pebler, *Organometallics* **1999**, *18*, 3273. Trovacene = ($\eta^7$-**tro**pylium)**va**nadium($\eta^5$-**c**yclop**en**tadi**e**nyl); the number in square brackets preceding the name indicates the site of substitution: [5]trovacene is functionalized at the five-membered ring, [7]trovacene at the seven-membered ring.

[2] For a case study, as well as for leading references to the field in general, see: J. A. McCleverty, M. D. Ward, *Acc. Chem. Res.* **1998**, *31*, 842.

[3] C. Elschenbroich, P. Kühlkamp, A. Behrendt, K. Harms, *Chem. Ber.* **1996**, *129*, 859.

[4] [4a] C. Elschenbroich, J. Heck, *J. Am. Chem. Soc.* **1979**, *101*, 6773. − [4b] C. Elschenbroich, J. Heck, *Angew. Chem. Int. Ed. Engl.* **1981**, *20*, 267. − [4c] C. Elschenbroich, J. Heck, F. Stohler, E. Bilger, *Chem. Ber.* **1984**, *117*, 23. − [4d] C. Elschenbroich, G. Heikenfeld, M. Wünsch, W. Massa, G. Baum, *Angew. Chem.* **1988**, *100*, 397; *Angew. Chem. Int. Ed. Eng.* **1988**, *27*, 414. − [4e] C. Elschenbroich, A. Bretschneider-Hurley, J. Hurley, W. Massa, S. Wocadlo, J. Pebler, E. Reijerse, *Inorg. Chem.* **1993**, *32*, 5421. − [4f] C. Elschenbroich, T. Isenburg, B. Metz, A. Behrendt, K. Harms, *J. Organomet. Chem.* **1994**, *481*, 153. − [4g] C. Elschenbroich, B. Metz, B. Neumüller, E. Reijerse, *Organometallics* **1994**, *13*, 5072. − [4h] C. Elschenbroich, A. Bretschneider-Hurley, J. Hurley, A. Behrendt, W. Massa, S. Wocadlo, E. Reijerse, *Inorg. Chem.* **1995**, *34*, 743. − [4i] C. Elschenbroich, T. Isenburg, A. Behrendt, *Inorg. Chem.* **1995**, *34*, 6565.

[5] [5a] O. Schiemann, Dissertation, Philipps-Universität, Marburg, Germany, **1998**. − [5b] J. Plackmeyer, Diploma, Philipps-Universität, Marburg, Germany, **1997**. − [5c] M. Wolf, Dissertation, Philipps-Universität, Marburg, Germany, **1999**.

[6] [6a] R. B. King, F. G. A. Stone, *J. Am. Chem. Soc.* **1959**, *81*, 5263. − [6b] G. Engebretson, R. Rundle, *J. Am. Chem. Soc.* **1963**, *85*, 481. − [6c] W. M. Gulick, Jr., D. H. Geske, *Inorg. Chem.* **1967**, *6*, 1320.

[7] [7a] E. W. Post, R. G. Cooks, J. C. Kotz, *Inorg. Chem.* **1970**, *9*, 1670. − [7b] T. López, A. Campero, *J. Organomet. Chem.* **1989**, *378*, 91. − [7c] B. Wrackmeyer, U. Dörfler, W. Milius, M. Herberhold, *Z. Naturforsch.* **1995**, *50b*, 201.

[8] C. J. Groenenboom, H. J. Liefde Meijer, F. Jellinek, *Recl. Trav. Chim. Pays. Bas* **1974**, *93*, 6.

[9] C. J. Groenenboom, H. J. Liefde Meijer, F. Jellinek, *J. Organomet. Chem.* **1974**, *69*, 235.

[10] A. Schulz, W. Kaim, *Chem. Ber.* **1989**, *12*, 1863.

[11] F. Zettler, H. D. Hansen, H. Hess, *J. Organomet. Chem.* **1974**, *72*, 157. − J.F. Blount, F. Finocchiaro, D. Gust, K. Mislow, *J. Am. Chem. Soc.* **1973**, *95*, 7019.

[12] J. B. Flanagan, S. Margel, A.J. Bard, F. C. Anson, *J. Am. Chem. Soc.* **1978**, *100*, 4248.

[13] J. D. Kennedy in *Multinuclear NMR* (Ed.: J. Mason), Plenum Press, New York, **1987**, chapter 8. − H. Nöth, B. Wrackmayer, *Nuclear Magnetic Resonance Spectroscopy of Boron Compounds*, Springer, Berlin, **1978**, chapter 8.

[14] Access to the extensive literature on organic triradicals is provided by: [14a] H. Nishide, M. Miyasaka, E. Tsuchida, *Angew. Chem. Int. Ed.* **1998**, *37*, 2400. − [14b] A. Rajca, J. Wongsriratanakul, S. Rajca, *J. Am. Chem. Soc.* **1997**, *119*, 11674. − [14c] K. R. Stickley, T. D. Selby, S. C. Blackstock, *J. Org. Chem.* **1997**, *62*, 448. − [14d] J. Fujita, M. Tanaka, H. Suemune, N. Koga, K. Matsuda, H. Iwamura, *J. Am. Chem. Soc.* **1996**, *118*, 9347. − [14e] J. Veciano, C. Rovira, N. Ventosa, M. I. Crespo, F. Palacio, *J. Am. Chem. Soc.* **1993**, *115*, 57. − [14f] A. Raja, *Chem. Rev.* **1994**, *94*, 871. − [14g] H. Iwamura, *Adv. Phys. Org. Chem.* **1990**, *26*, 179. − [14h] Landolt−Börnstein, *Magnetic Properties of Free Radicals*, New Series, II/9, Part d2, Springer, Berlin, **1980**. − [14i] H. Iwamura, K. Inoue, T. Hayamizu, *Pure Appl. Chem.* **1996**, *68*, 243. − [14j] W. M. Nan, *Angew. Chem. Int. Ed. Engl.* **1997**, *36*, 2445. − [14k] T. Itoh, K. Matsuda, H. Iwamura, *Angew. Chem.* **1999**, *111*, 1886; *Angew. Chem. Int. Ed.* **1999**, *38*, 1791.

[15] For examples from inorganic chemistry/coordination chemistry, see: [15a] V. A. Ung, A. M. W. Cargill Thompson, D. A. Bardwell, D. Gatteschi, J. C. Jeffery, J. A. McCleverty, F. Totti, M. D. Ward, *Inorg. Chem.* **1997**, *36*, 3447. − [15b] P. B. Hitchcock, D. L. Hughes, L. F. Larkworthy, G. J. Leigh, C. J. Marmion, J. R. Sanders, G. W. Smith, J. S. de Souza, *J. Chem. Soc., Dalton Trans.* **1997**, 1127. − [15c] I. Shweky, L. E. Pence, G. C. Papaefthymion, R. Sessoli, J. W. Yun, A. Bino, S. J. Lippard, *J. Am. Chem. Soc.* **1997**, *119*, 1037. − [15d] O. Kahn, *Molecular Magnetism,* VCH, Weinheim, **1993**, chapter 10. − [15e] J. K. McCusker, C. A. Christmas, P. M. Hagen, R. J. Chadha, D. F. Harvey, D. N. Hendrickson, *J. Am. Chem. Soc.* **1991**, *113*, 6114. − [15f] M. Tanaka, K. Matsuda, T. Itoh, H. Iwamura, *Angew. Chem.* **1998**, *110*, 866; *Angew. Chem. Int. Ed.* **1998**, *37*, 810.

[16] To the best of our knowledge the only organometallic triradicals which have been isolated are cyanuratotris[bis($\eta^5$-methylcyclopentadienyl)titanium(III)][19] and 1,3,5-tri([5]trovacenyl)benzene.[5a] Formally, certain paramagnetic termetallocene cations, generated during electrochemical oxidations in CV experiments,[21] also belong to this class.

[17] Equation 2 was derived from the more general expression valid for an equilateral triangular configuration with nonidentical coupling pathways, described by the parameters $J$ and $J'$, where the ratio $J'/J = \alpha$ was set to one (see Ref.[14d]). Apart from the structural information about **7**$^{+\cdot\cdot\cdot}$, gathered by X-ray crystallography, the simplification inherent in Equation 2 is justified by the fact that the fit based on the more general expression given in Ref.[14d] was optimal for $\alpha = 1$.
[18] A. Raja, *Chem. Rev.* **1994**, *94*, 871.
[19] R. D. Cannon, R. P. White, *Progr. Inorg. Chem.* **1988**, *36*, 195. − S. J. Lippard, *Angew. Chem. Int. Ed. Engl.* **1988**, *27*, 344. H. Y. Woo, H. So, M. T. Pope, *J. Am. Chem. Soc.* **1996**, *118*, 621.
[20] B. F. Fieselmann, D. N. Hendrickson, G. D. Stucky, *Inorg. Chem.* **1978**, *17*, 1841.
[21] See: S. Barlow, D. O′Hare, *Chem. Rev.* **1997**, *97*, 637, for leading references.
[22] C. Elschenbroich, S. Voss, O. Schiemann, A. Lippek, K. Harms, *Organometallics* **1998**, *17*, 4417.
[23] A. Pelter, K. Smith, H. C. Brown, *Borane Reagents*, Academic Press, London, **1988**.

Received July 15, 1999
[I99261]